Draft version April 20, 2015
Preprint typeset using LaTeX style emulateapj v. 12/16/11

DETECTING ACTIVE ASTEROIDS/COMETS FROM OSSOS SURVEY IMAGES

Authors
Affiliations
Draft version April 20, 2015

ABSTRACT

Abstract.
Keywords: keywords

1. INTRODUCTION

Until the last decade, comets and asteroids have been thought of as separate populations differing both in morphology and dynamics. With different fractions of volatile content, an obvious differentiator is the presence of a transient coma and/or tail, whereas asteroids exhibit bare nuclei photometric properties. [fill in: mention Tisserand parameter here?] With the recent advent of large wide-field surveys which have regularly monitored large populations of solar system objects, objects which exist between the classification of comets and asteroids have been identified in steady numbers. The classical view of comets being primarily icy bodies with highly eccentric orbits, and asteroids being primarily rocky bodies with stable orbits confined to the main asteroid belt between Mars and Jupiter (Sheppard and Trujillo 2015), has been usurped by the discovery of comet-asteroid transition objects. With the discovery of asteroids in dynamically cometary orbits, dynamically asteroidal objects that exhibit burst of cometary activity or are associated with meteor streams such as the Damocloids (Sonnett et al. (2011); and references therein, Gilbert and Wiegert (2009)) the classification criteria for asteroids and comets has become less obvious. Objects such as these may be comets which have exhausted their volatile content or are dormant, or asteroids which have a higher volatile fraction. In this study we focus on the 'active asteroids' (AAs) (or main belt comets (MBCs)), which are a population of bodies with stable asteroid-like main belt orbits that exhibit transient comae or tails consistent with cometary morphology. As it is expected that objects which are in the inner solar system would have long ago sublimated their ice away, the active asteroids pose an interesting insight to the heliocentric distance at which ice condenses, known as the 'snow line', which of interest to planetary formation and determining the chemistry of the early solar nebula.

For objects which formed in the the outer region of the main belt, the crystallized water ice which was present at the time of formation and not exposed to primordial heating may still remain in reservoirs beneath the surface (Prialnik and Rosenberg 2009). According to models developed by Fanale and Salvail (1989), beyond heliocentric distances of 2.4 AU ice can be protected against sublimation by a relatively thin surface regolith of depth 1 – 100 m for the entire age of the solar system. If the ice layer were to be exposed to sub solar heating, sublimation could be triggered which would eject dust particles from the surface producing a coma [todo: check that wording not too similar to paper]. The source of the dust emission may be different for each object and could include ice sublimation, impact ejecta, rotational instabilities due to YORP torques, or a combination of several effects. (Hsieh et al. (2015); and references therein).

Since the first discovery of an active main-belt asteroid, 133P/Elst-Pizarro (Elst et al. 1996), several attempts have been made to identify new objects of this type; at present, eighteen objects have been identified (Figure 1) [todo: check figure reference] (Jewitt et al. 2015). A comprehensive review of these surveys can be found in Hsieh et al. (2015). A persistent challenge to this effort is that the detection of the faint coma or tails around small dark objects is highly dependent on the magnitude constraints of the survey. As most asteroids fall near the limiting magnitude of the survey in which they are discovered [todo: citation necessary?], objects which are larger, closer, or have higher albedo are preferentially detected and any dust emission would be more easily apparent. At present, the active fraction of identified active asteroids greater than 1 km to main belt asteroids greater than 1 km is $f \sim 10^5$, and describes a strong lower limit as many objects are yet undetected. (Jewitt et al. 2015)

In this paper, we present a study using the Canada-France-Hawaii Telescope (CFHT) Outer Solar System Origins Survey (OSSOS) data to identify the presence of cometary activity in previously discovered asteroids. We select the Hungaria family as the test group for our search pipeline. Previously undetectable emission activity may be able to be identified in the OSSOS survey, which was designed to detect trans neptunian objects and as such has a limiting magnitude that is much lower than previous surveys (Hsieh et al. 2015). The survey covers a wide field of both the ecliptic plane and low inclinations allowing for the observation of a large number of main belt objects in different orbital phase spaces. In this study we identify all observations of previously discovered main belt objects in the OSSOS data set, and identify potential activity by measuring the asteroidal brightness profile and comparing this to a stellar model profile in order to detect a large deviation in width potentially characteristic of a coma or jet around the asteroid. This is similar to the process employed by Luu (1992) and Sonnett, Kleyna, Jedicke, and Masiero (2011).

2. OBSERVATIONS

Observations taken by OSSOS with the CFHT MegaPrime wide-field optical imaging facility at the summit of Mauna Kea, Hawaii, have been collected since 2013. The wide-field imager, MegaCam, consists of a 36

CCD image plane, each 2048 x 4125 CCD with resolution of 0.185"/pix. This covers a field of roughly 1° x 1° on the sky. Each block of data taken consists of a mosaic of 21 segments of one-square-degree sky coverage, and at present, covers two orbital phase spaces on the plane of the ecliptic, and two off plane at low inclinations. The OSSOS survey employs the u* and r' filters on the MegaCam with integration times of 287, 387, and 500 seconds, yielding a lower limit of 24.5 magnitudes.

The OSSOS images are reduced via the moving object pipeline (MOP). [todo: how reduced]. (standard data detrending???) Source characteristic measurements were obtained from source extraction (SEP 2015) and were used to extract the orbital information the transient object.

3. ANALYSIS

From the calculated arcs provided by SSOIS (Gwyn et al. 2012) of main belt objects in the AstDys catalogue (AstDys 2015) we were able to predict which asteroids were present in the OSSOS data set and could be examined for cometary activity. From a set of 3528 images, there are [todo: fill in] observations of [todo: fill in] asteroids in the OSSOS data. We analyze a small group of objects in the Hungaria family as our test case for our automated pipeline. Of the 1187 Hungarias we have 76 observations of 25 objects.

3.1. *Object identification*

An automated pipeline was written to identify each asteroid in an OSSOS exposure by: location relative to the predicted coordinates, elongation due to trailing effects caused by the apparent rate of motion over the duration of the exposure, and apparent magnitude.

The coordinates of each object in the exposure were obtained from the photometric software (SEP 2015), and objects which were closest to the predicted location (at the midpoint of the exposure) as calculated by known arc (JPL 2015) [todo: is this citation necessary?] were chosen as candidate objects. If no objects were detected within a set radius calculated from the uncertainty in the asteroid arc, the radius was increased by a factor of 1.5 and the search was repeated.

The expected elongation of the trail was calculated from the predicted motion of the asteroid over the length of the exposure (JPL 2015) under the assumption of constant motion. This value was then compared to the elliptical shape parameters measured by the photometry for each candidate object. A difficulty in this process is that objects which are moving faster during the exposure, and thus trailed to a greater extent, will be less elliptical in shape. As the photometry is optimized for point sources and extended sources such as galaxies, the accuracy of the shape parameters is correlated to the extent of the elongation. For this reason we implement an error of 20 percent on the measurement of the semi-major and semi-minor axis reported by the photometry. [to do: be more specific about why 20?] For objects which appear very elongated, typically spanning 30 pixels end-to-end, the photometry incorrectly resolves the asteroid as two separate objects. In this case both objects would meet all the criteria conditions. In order to not pass such objects through the pipeline, if multiple objects met all the conditions, the objects were removed from the pipeline and flagged for review.

The inability of the photometry software to correctly measure the shape of the asteroid trail will also have an effect on the measured flux as the aperture may not include the total amount of light. As the centre of the object is determined by the flux weighted barycenter of the object, this may also result in an inaccurate measurement of the astrometry. In order to avoid this error, the centre coordinates of the object were chosen as the centre of the elliptical aperture for fast-moving objects. In addition, the elongation effect in itself may affect the accuracy of the flux measurement without taking into account the potential loss of light. This is a result of the flux being spread over a larger area than the point spread function (PSF), which reduces the per unit area apparent magnitude and the signal-to-noise (Vereš et al. 2012). A direct consequence is a lowered limiting magnitude for fast moving asteroids. A third consideration is that objects which are active and have jets or a coma will appear brighter than the expected magnitude calculated from previous observations. Depending on the extent of the activity, this could cause the object to be measured as several magnitudes greater than predicted. For this reason we did not exclude objects which were brighter than expected. For these reasons, in subjecting the candidate object to a consistency check with the predicted value we used an uncertainty of at least 2 magnitudes, and did not reject the object if it was inconsistent.

In order to accurately measure the PSF of the asteroid – which is necessary to check for anomalous flux surrounding the object that could indicate activity – it is necessary to ensure that the asteroid is isolated from other sources. In order to reject asteroids which were involved with background objects, the coordinates of the object were compared to a catalogue of bright sources built for the OSSOS data set. This will not, however, detect if the asteroid is involved with a faint background source nor a transient object such as a cosmic ray. It is possible that the involvement would cause the object to be rejected based on the measured elongation or shape.

A candidate object which did not meet any of the criteria mentioned above would be rejected. This would include objects which were involved with or too close to bad pixels or cosmic rays, on the edge of the CCD, in a diffraction ring of a nearby bright star (but far enough spatially to not be rejected as involved), or that could not be accurately measured by the photometry software.

Applying this identification process left 49 exposures of 19 asteroids to be examined.

3.2. *PSF comparison*

A postage stamp of size 2.5 times the full-width-half-maximum (FWHM) and centred on the midpoint of the elongated shape was rotated such that asteroid trail was aligned parallel to the pixel rows on the CCD chip. The asteroid profile was averaged over the entire length of the postage stamp. The stellar model PSF was built from the OSSOS MOP at the location of and with the same magnitude as the asteroid on the CCD to account for any distortion, and rotated by the same angle. The profile was measured as the average over the width of the model star. A 3 sigma difference between the subtracted profiles was used to indicate the presence of additional

Table 1
Rejection cause for images through identification pipeline

Total number of images	76
Rejection cause	**# images**
Involved with background stars	1
Incorrectly resolved as two objects	5
Did not meet elongation or magnitude criteria	2
Incorrectly measured by the photometry	5
Could not be processed by the photometry software	6
Off the edge of the CCD	5
In saturated region of nearby bright star	2
Could not be resolved from the background	1
Bad exposure	0
Retained	49

flux around an asteroid, characteristic of a cometary comae. There were [fill in] asteroids which were measured to be above this limit and were flagged for visual confirmation. Due to saturation effects, asteroids with magnitudes greater than 18.5 were not analyzed for activity. However, as previous surveys have included this set of objects (Hsieh et al. 2015) we were comfortable with this exclusion.

3.3. *Detection Efficiency*

How well do we identify coma vs jets vs tails ? How may do we detect vs observed? What are the statistics? Why are the results so bad?

4. DISCUSSION

5. PHOTOMETRY ERRORS

All objects which were successfully identified passed the elongation condition How many objects were 'very' elongated?

As the involvement check was preformed using a catalogue of bright objects, it is possible that some asteroids identified and carried through the pipeline process were involved with dim background objects. An example of this is shown in figure 3. Depending on the geometry of the involvement this could be selected as an asteroid with activity, possibly a large bright jet. In order to distinguish between activity and involvement, the asteroids with unusual PSF's were all manually reviewed. Through this process we could determine whether a jet was present, in which case the outflowing dust would also have a trailing effect through the exposure, or if it were a case of involvement. We do not expect that a jet would be present for a fraction of the exposure time during one observation.

6. RECOMMENDATIONS

Use a trail fitting function for improved photometry on fast moving objects such as described by Vereš et al. (2012). Tail detection pipeline like Sonnett et al. (2011)

Acknowledgments.

REFERENCES

AstDys, 2015. URL http://hamilton.dm.unipi.it/astdys/index.php?pc=5.

E. W. Elst, O. Pizarro, C. Pollas, J. Ticha, M. Tichy, Z. Moravec, W. Offutt, and B. G. Marsden. Comet P/1996 N2 (Elst-Pizarro). IAU Circ., 6456:1, August 1996.

F. P. Fanale and J. R. Salvail. The water regime of asteroid (1) Ceres. Icarus, 82:97–110, November 1989. doi:10.1016/0019-1035(89)90026-2.

A. M. Gilbert and P. A. Wiegert. Searching for main-belt comets using the Canada-France-Hawaii Telescope Legacy Survey. Icarus, 201:714–718, June 2009. doi:10.1016/j.icarus.2009.01.011.

S. D. J. Gwyn, N. Hill, and J. J. Kavelaars. SSOS: A Moving-Object Image Search Tool for Asteroid Precovery. PASP, 124:579–585, June 2012. doi:10.1086/666462.

H. H. Hsieh, L. Denneau, R. J. Wainscoat, N. Schörghofer, B. Bolin, A. Fitzsimmons, R. Jedicke, J. Kleyna, M. Micheli, P. Vereš, N. Kaiser, K. C. Chambers, W. S. Burgett, H. Flewelling, K. W. Hodapp, E. A. Magnier, J. S. Morgan, P. A. Price, J. L. Tonry, and C. Waters. The main-belt comets: The Pan-STARRS1 perspective. Icarus, 248:289–312, March 2015. doi:10.1016/j.icarus.2014.10.031.

D. Jewitt, H. Hsieh, and J. Agarwal. The Active Asteroids. *ArXiv e-prints*, February 2015.

JPL, 2015. URL http://hamilton.dm.unipi.it/astdys/index.php?pc=5.

J. X. Luu. High resolution surface brightness profiles of near-earth asteroids. Icarus, 97:276–287, June 1992. doi:10.1016/0019-1035(92)90134-S.

D. Prialnik and E. D. Rosenberg. Can ice survive in main-belt comets? Long-term evolution models of comet 133P/Elst-Pizarro. MNRAS, 399:L79–L83, October 2009. doi:10.1111/j.1745-3933.2009.00727.x.

SEP, 2015. URL http://sep.readthedocs.org/en/v0.3.x/.

S. S. Sheppard and C. Trujillo. Discovery and Characteristics of the Rapidly Rotating Active Asteroid (62412) 2000 SY178 in the Main Belt. AJ, 149:44, February 2015. doi:10.1088/0004-6256/149/2/44.

S. Sonnett, J. Kleyna, R. Jedicke, and J. Masiero. Limits on the size and orbit distribution of main belt comets. Icarus, 215: 534–546, October 2011. doi:10.1016/j.icarus.2011.08.001.

The International Astonomical Union, 2015. URL http://www.minorplanetcenter.net/iau/MPCORB.html.

P. Vereš, R. Jedicke, L. Denneau, R. Wainscoat, M. J. Holman, and H.-W. Lin. Improved Asteroid Astrometry and Photometry with Trail Fitting. PASP, 124:1197–1207, November 2012. doi:10.1086/668616.

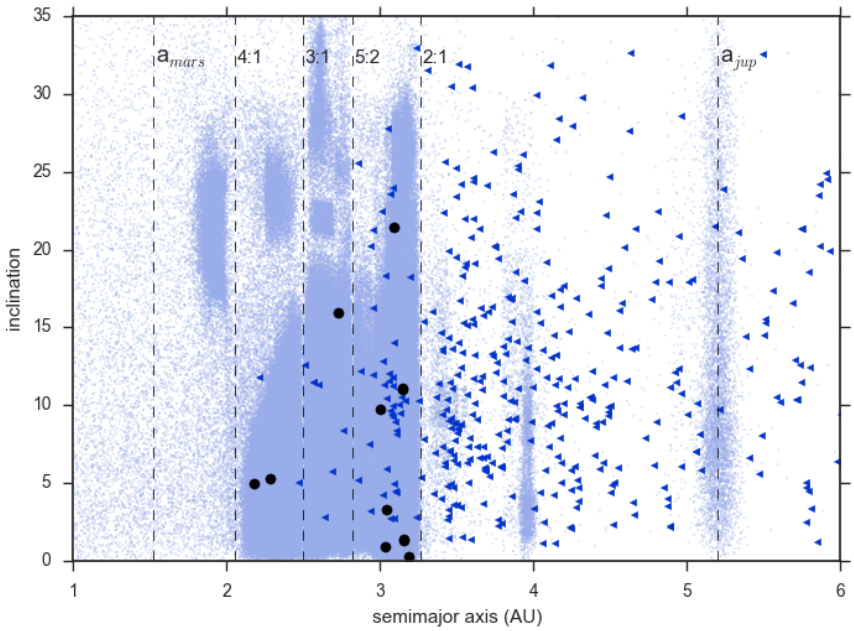

Figure 1. Inclination of all known objects in the main asteroid belt as a function of semimajor axis. Mean motion resonances between Mars and Jupiter as well as the planet's semimajor axis are marked in dashed lines, main belt objects are marked as light small dots, comets as arrows, and active asteroids as stars. Union (2015)